ELSEVIER

Soil Dynamics and Earthquake Engineering 18 (1999) 209–228

SOIL DYNAMICS AND EARTHQUAKE ENGINEERING

Modeling, synthetics and engineering applications of strong earthquake wave motion[1]

Masanobu Shinozuka[a,*], George Deodatis[b], Ruichong Zhang[c], Apostolos S. Papageorgiou[d]

[a]*Department of Civil Engineering, University of Southern California, Los Angeles, CA90089-2531, USA*
[b]*Department of Civil Engineering and Operations Research, Princeton University, Princeton, NJ 08544, USA*
[c]*Division of Engineering, Colorado School of Mines, Golden, CO 80401, USA*
[d]*Department of Civil and Environmental Engineering, Rensselaer Polytechnic Institute, Troy, NY 12180-3590, USA*

Received 10 January 1997; received in revised form 22 September 1998; accepted 22 September 1998

Abstract

State of the art in modeling, synthetics, statistical estimation, and engineering applications of strong ground motion is reported in this paper. In particular, models for earthquake wave motion are presented, in which uncertainties both in the earth medium and the seismic source are taken into consideration. These models can be used to synthesize realistic strong earthquake ground motion, specifically near-field ground motion which is quite often not well recorded in real earthquakes. Statistical estimation techniques are also presented so that the characteristics of spatially-correlated earthquake motion can be captured and consequently used in investigating the seismic response of such large scale structures as pipelines and long-span bridges. Finally, applications of synthesized strong ground motion in a variety of engineering fields are provided. Numerical examples are shown for illustration.

Keywords: Seismic source mechanism; Earthquake wave motion model; Synthetics of earthquake motion; Non-homogeneous medium; Discrete wave number method; Statistical estimation; Loma prieta earthquake; Near-field ground motion

1. Introduction

Earthquake ground motion is the result of seismically propagating waves in the earth medium, which originate at a seismic source. Therefore, the establishment of realistic models for the earth medium and the seismic source plays a crucial role in strong earthquake ground motion synthesis, which provides fundamental information for the aseismic design of structures. The first part of this paper is devoted to the exploration of realistic models for the earth medium and the seismic source. Uncertainties in both the earth medium and the seismic source are taken into consideration so that the stochastic nature of earthquake ground motion can be captured in the synthetics. As one application of these earthquake models, near-field ground motion, which is usually not well recorded in real earthquakes, is synthesized. The synthesized near-field ground motion can then be used to analyze the effects of various parameters of the seismic source (such as rupture pattern, slip distribution and directivity) and of the earth medium (such as the irregular topography and laterally non-homogeneous medium properties) on the response spectra. Consequently, the physical and engineering significance of the effects of these parameters can be estimated. This can be useful for decision-makers trying to establish whether current seismic codes and retrofit guidelines are adequate.

The second part of this paper deals with an important engineering application of synthesized seismic ground motion: the estimation of statistics such as the frequency-wave number (F-K) spectrum and the coherence function which characterize the temporal and spatial variations of strong ground motion. These statistics can then be used to simulate spatially-correlated earthquake ground motions, which can be conveniently used for earthquake-resistant structural design, especially for elongated structures such as pipelines and long-span bridges.

2. Modeling of earthquake wave motion

An earthquake is a sudden motion of the ground caused by seismic waves that are generated by the abrupt rupture of

[1] This paper is developed primarily on the basis of the review paper entitled 'Stochastic Process Modeling and Simulation of Strong-Ground-Motion Accelerations' authored by M. Shinozuka and presented in Emilio Rosenblueth Seminar at the Eleventh World Conference on Earthquake Engineering in Acapulco, Mexico on June 23–28, 1996.

* Corresponding author.

0267-7261/99/$ - see front matter
PII: S0267-7261(98)00045-1

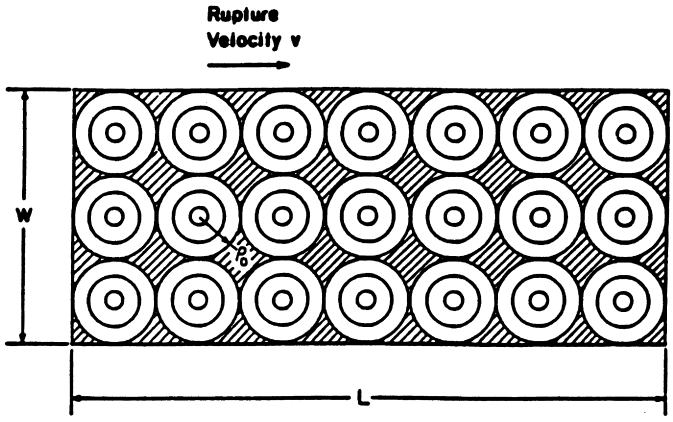

Fig. 1. The specific barrier model proposed by Papageorgiou and Aki [28].

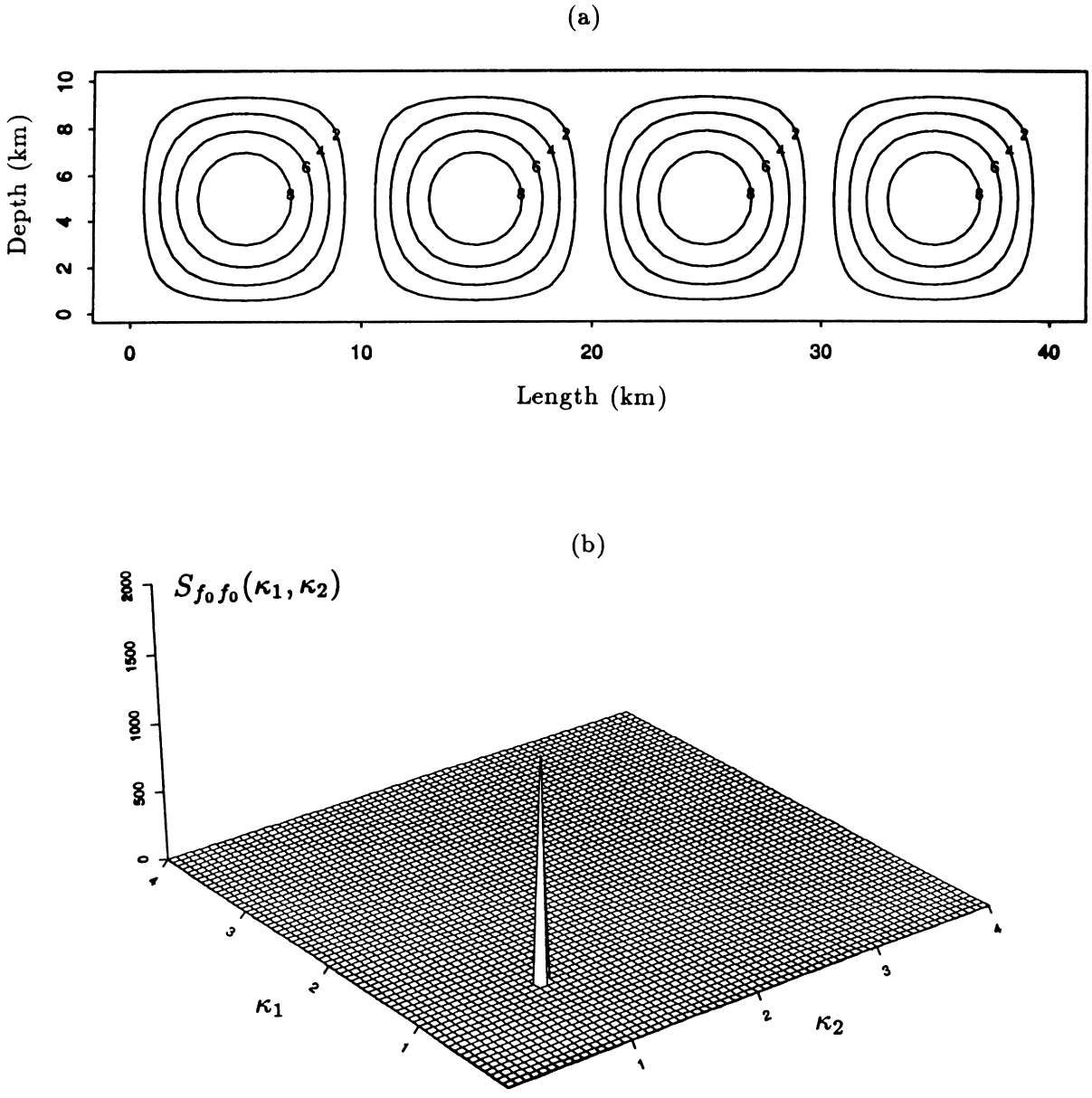

Fig. 2. (a) Contours for the distribition of the final slip of the underlying barrier model with regular circular-type cracks; (b) corresponding power spectral density function used to obtain the final slip distribution.

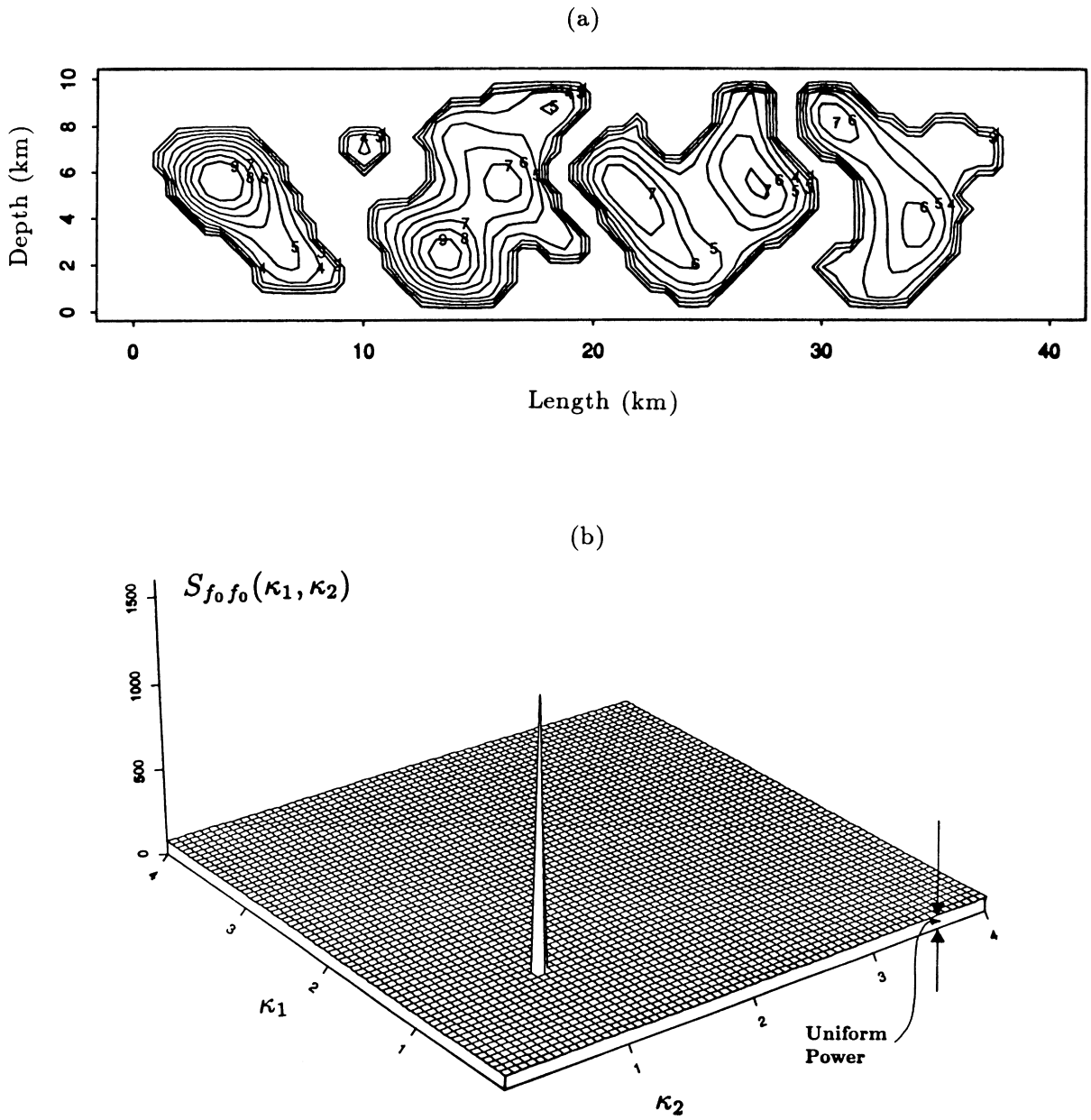

Fig. 3. (a) Contours for the distribution of the final slip of the barrier model with irregular boundaries; (b) corresponding power spectral density function used to obtain the final slip distribution.

a fault. Since major earthquakes pose one of the greatest natural hazards facing humankind, numerous efforts have been made by seismologists, geophysicists, structural and geotechnical engineers, among others, to explore their fundamental mechanism from the scientific point of view, and to mitigate their hazard from the engineering point of view.

Since earthquake motion is the result of propagating seismic waves through the earth medium originally generated at the seismic source, realistic modeling of the earth medium and the seismic source becomes particularly important for accurately synthesizing earthquake wave motion. Some recent developments in these areas are described in the following.

2.1. Modeling of seismic source

The assumption of a point source is acceptable when computing seismic ground motion in the far field. However, when near field ground motion is to be synthesized, it is necessary to consider an extended seismic source. An extended seismic source is usually described as a slip (dislocation) rupturing over a certain area of a fault. The evolution of the slip as a function of time and the distribution of the final slip values over the seismic fault can be either assumed using physical models of the source, or obtained using earthquake ground motion records to solve the inverse problem. The former approach is referred to in this paper as the

physically-consistent source model, while the latter as the seismologically consistent source model.

2.1.1. Physically-consistent source model

One of the best available models for the description of the rupture of an extended seismic source is the specific barrier model introduced by Papageorgiou and Aki [28]. According to this model, a rectangular seismic fault is assumed to rupture consecutively in a series of circular sub-faults (cracks) separated by unbroken barriers, as indicated in Fig. 1. The rupture begins at the center of each circular crack and propagates radially with a prescribed rupture velocity. When the rupture reaches the circumference of the circular sub-fault (barrier), a healing front is initiated propagating radially from the circumference toward the center with a prescribed healing velocity. At the instant the healing front reaches a given point within the circular crack, the rupture at this point stops, fixing the final dislocation (slip) at that position.

In a recent paper [10], a barrier model with irregular boundaries has been introduced to describe more realistically the roughness of the boundaries as observed in actual seismic events. In that paper, the distribution of the final slip over the area of the seismic fault was given without an explanation of how it was computed. In the following, the methodology to establish the barrier model with irregular boundaries is presented for the first time. It is based on a series of private communications between G. Deodatis and A.S. Papageorgiou in January 1995.

The basic idea is that an underlying barrier model with regular circular-type boundaries [28] is transformed into a corresponding one with irregular boundaries using the spectral representation method for simulation of stochastic fields [32]. Contours for the distribution of the final slip of an underlying barrier model with 4 regular circular-type cracks is shown in Fig. 2a. Note that these 4 cracks are not perfectly circular since they are obtained as a realization of a stochastic field with the power spectral density function shown in Fig. 2b, using the spectral representation formula:

$$f(x_1,x_2)=|\sqrt{2}\sum_{n_1=0}^{N_1-1}\sum_{n_2=0}^{N_2-1}\sqrt{2S_{f_0f_0}(\kappa_{1n_1},\kappa_{2n_2})\Delta\kappa_1\Delta\kappa_2}\times[\cos(\kappa_{1n_1}x_1+\kappa_{2n_2}x_2+\Phi^{(1)}_{n_1n_2})+\cos(\kappa_{1n_1}x_1-\kappa_{2n_2}x_2+\Phi^{(2)}_{n_1n_2})]| \quad (1)$$

where f is the stochastic field modeling the final slip, x_1 and x_2 are space coordinates, $S_{f_0f_0}$ is the power spectral density function of the field, κ_1 and κ_2 are wave numbers, $\Phi^{(1)}_{n_1n_2}$ and $\Phi^{(2)}_{n_1n_2}$ are random phase angles uniformly distributed between 0 and 2π, and:

$$\kappa_{1n_1}=n_1\Delta\kappa_1;\ \kappa_{2n_2}=n_2\Delta k_2 \quad (2)$$

$$\Delta\kappa_1=\frac{\kappa_{1u}}{N_1};\ \Delta k_2=\frac{\kappa_{2u}}{N_2} \quad (3)$$

with κ_{1u} and κ_{2u} being the upper cutoff wave numbers. For more information about the two-dimensional spectral representation formula shown in Eq. (1), the reader is referred to Ref. [32].

Using Eq. (1) and the delta function power spectrum shown in Fig. 2b, the final slip distribution shown in Fig. 2a is obtained. As mentioned earlier, although the 4 cracks shown in Fig. 2a have regular boundaries, these boundaries are not perfectly circular because of Eq. (1).

In order now to produce the final slip distribution of the corresponding barrier model with irregular boundaries, the delta function power spectrum shown in Fig. 2b is modified by adding a low-level uniform power throughout the entire wave number domain, as indicated in Fig. 3b. Using then Eq. (1) and the new power spectral density function shown in Fig. 3b, the contours of the final slip distribution of the corresponding barrier model with irregular boundaries are computed and plotted in Fig. 3a.

Although Fig. 3a shows cracks with particularly irregular boundaries, the basic characteristics of the corresponding regular cracks shown in Fig. 2a are preserved: their number (4) and their overall dimensions. In addition, the slip distribution shown in Fig. 3a can be easily normalized to have the same seismic moment as the one shown in Fig. 2a. It is believed that the barrier model with irregular boundaries describes the roughness of the boundaries of the cracks more realistically and in a fashion similar to the one observed in actual earthquakes.

Once the final slip distribution of the barrier model with irregular boundaries is established as shown in Fig. 3a, the evolution of the slip at every location as a function of time - described by the dislocation function $\Delta u(r,t)$- has to be determined. This is accomplished by modifying the expressions for $\Delta u(r,t)$ proposed by Papageorgiou and Aki [28] for the barrier model with circular boundaries. In this paper, the dislocation function at a distance r from the center of the circular crack at time instant t is defined as:

$$\Delta u(r,t)=C\sigma_e\frac{v_s}{\mu}\sqrt{t^2-\frac{r^2}{v^2}}H\left(t-\frac{r}{v}\right)\ for\ t<t_r \quad (4)$$

$$\Delta u(r,t)=C\sigma_e\frac{v_s}{\mu}\sqrt{t_r^2-\frac{r^2}{v^2}}\ for\ t>t_r \quad (5)$$

with:

$$t_r=\frac{r_0}{v}+\frac{r_0-r}{v_h} \quad (6)$$

where C is a parameter depending on the shear wave velocity and the rupture velocity, σ_e is the effective stress, v is the rupture velocity, v_s is the shear wave velocity, v_h is the healing velocity, μ is the rigidity of the medium, r_0 is the radius of the circular crack, t_r is the rise time and H is Heavyside's unit step function. There is no analytical expression for the Fourier transform $F(\omega)$ of the expression shown in Eqs. (4) and (5). This Fourier transform can be

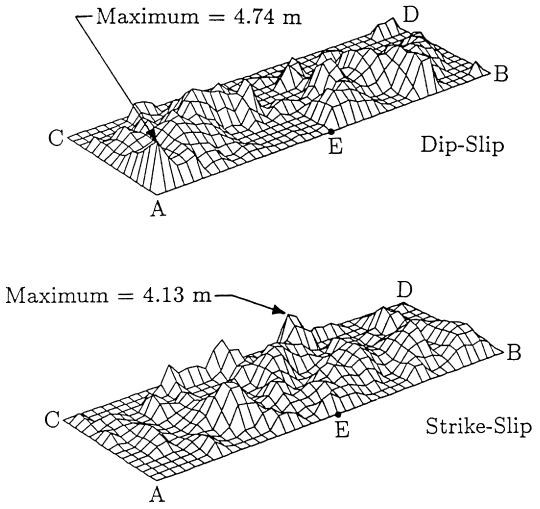

Fig. 4. Slip distribution over a rectangular fault in a seismologically consistent Loma Prieta earthquake source model [40].

be simplified as:

$$F(\omega)=\frac{C\sigma_e v_s}{\Delta u_F \omega^2 \mu}\sqrt{\frac{r_0{}'+r}{r_0{}'-r}}\exp\left(\frac{-i\omega r}{v}\right)\times\left[\exp\left(\frac{-i\omega(r_0{}'-r)}{v}\right)-1\right]+\pi\delta(\omega) \tag{9}$$

with:

$$r_0{}'=t_r v;\ r=r_0-\left(t_r-\frac{r_0}{v}\right)v_h. \tag{10}$$

Denoting now by Δu the following ratio:

$$\Delta u=\frac{\Delta u_f}{\Delta u_F^{center}} \tag{11}$$

where Δu_f^{center} is the final slip at the center of the crack, it can be shown that Δu and t_r are related as:

$$t_r=\frac{\frac{-2r_0 v_h}{v^2}\left(1+\frac{v_h}{v}\right)+\sqrt{4r_0^2\left(1+\frac{v_h}{v}\right)\left[\left(1+\frac{v_h}{v}\right)\frac{1}{v^2}+\Delta u^2\left(1-\frac{v_h}{v}\right)\left(\frac{1}{v}+\frac{1}{v_h}\right)^2\right]}}{2\left(1-\frac{v_h^2}{v^2}\right)} \tag{12}$$

approximated, however, by a series of n_s line segments, leading to the expression:

$$F(\omega)=\frac{C\sigma_e v_s}{\Delta u_F \mu v}\left[\frac{1}{i\omega}\exp\left(-i\omega\frac{r_0{}'}{v}\right)\sqrt{r_0'^2-r^2}+\sum_{k=1}^{n_s}\left\{\frac{1}{i\omega}\left[\exp\left(-i\omega\frac{\rho_{k-1}}{v}\right)-\exp\left(-i\omega\frac{\rho_k}{v}\right)\right]\times\sqrt{\rho_{k-1}^2-r^2}+\left(\sqrt{\rho_k^2-r^2}-\sqrt{\rho_{k-1}^2-r^2}\right)\times\left[\frac{v}{\omega^2(\rho_k-\rho_{k-1})}\exp\left(-i\omega\frac{\rho_{k-1}}{v}\right)\times\left[\exp\left(-i\omega\frac{(\rho_k-\rho_{k-1})}{v}\right)-1\right]-\frac{1}{i\omega}\exp\left(-i\omega\frac{\rho_k}{v}\right)\right]\right\}\right]+\pi\delta(\omega) \tag{7}$$

where:

$$\rho_k=r+k\frac{r_0{}'-r}{n_s};\ r_o{}'=r_0+\frac{r_0-r}{v_h}v;\ k=0,1,\ldots,n_s \tag{8}$$

and Δu_F being the final slip at a distance r from the center of the circular crack. For $n_s=1$, the expression in Eq. (7) can

2.1.2. Seismologically-consistent source model

In contrast to the physically-consistent barrier model for the seismic source that can be used for actual as well as for scenario earthquake events, a seismologically-consistent model can be established for a specific earthquake by solving the inverse problem with the aid of earthquake ground motion records and wave propagation theory.

Both a seismologically-consistent source model and the corresponding synthesis of ground motion have been established for the 7.1 magnitude Loma Prieta earthquake that struck the San Francisco Bay area on October 17, 1989. One of the best seismologically-consistent source models was proposed by Zeng et al. [35,36] using the ray method and near field earthquake records (specifically 14 records within a 35 km radius around the epicenter). It should be noted that only direct arrivals of S waves are taken into account in the ray method adopted in the Zeng et al. work, for the sake of convenience and simplicity in computations. However, the results obtained through such an approach are acceptable from an engineering point of view as the direct propagating S waves dominate the seismic wave energy, compared to the energy carried by P waves and multi-reflected body waves. In addition, surface waves are not well developed in the near field.

The results of the Zeng et al. [35,36] analysis indicated a seismic source mechanism consisting of a bilaterally propagating shear slip over a rectangular fault with length of 40 km along the strike direction (130° clockwise from the

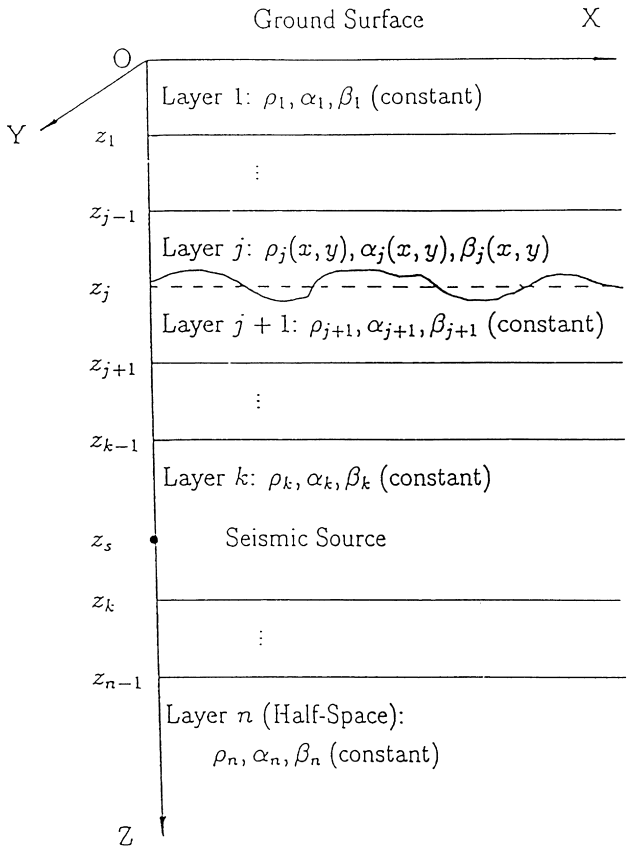

Fig. 5. Schematic diagram of layered half-space with a lateral non-homogeneities.

north direction) and width of 14 km along the dip direction (70° down from the horizontal). The final strike-slip and dip-slip distributions are plotted in Fig. 4.

In a recent paper, Zhang and Deodatis [40] successfully synthesized both near- and far-field Loma Prieta earthquake records using the seismologically-consistent source model proposed by Zeng et al. [35,36]. The earth model assumed in this work is based on geological profiles of the Santa Cruz mountain area and consists of three layers overlaying a half-space. Synthesized seismic ground motion from this work is presented later in this paper.

2.2. Earth medium modeling

In investigating seismic wave propagation and its correspondingly induced ground and/or underground motion responses, the earth is often modelled as a vertically non-homogeneous medium, idealized as a layered half-space with each layer being homogeneous. While this earth model is in general considered adequate to represent the basic characteristics of the real earth medium in pursuit of many engineering applications, the effects of lateral non-homogeneities of the earth medium (such as irregular surface, irregular interfaces and laterally non-homogeneous layer properties, see Fig. 5) on ground motion remain unknown qualitatively and quantitatively until the last two decades.

In reality, the earth medium can never be of perfectly lateral homogeneities and is always of stochastically lateral non-homogeneities to a certain extent (see e.g. [7,9,18]). It is apparent that not all of these lateral non-homogeneities are necessarily concerned in the earthquake wave motion model from the engineering point of view. This is thus related to a fundamental issue: whether or not a real laterally non-homogeneous earth medium can be approximated as laterally homogeneous when the seismic waves are under consideration.

Recently, Zhang et al. [38,41–43] investigated qualitatively and quantitatively the three-dimensional wave scattering phenomena in a layered half-space with lateral non-homogeneities under consideration. Their study shows that the introduction of lateral non-homogeneities into the earth medium model of a layered half-space results in the complexity of the problem not only mathematically but also physically. Specifically, when the irregular boundaries (surface and/or interfaces) and/or laterally non-homogeneous medium properties (wave speeds and density) are under consideration (see Fig. 5), wave scattering occurs due to these non-homogeneities, resulting in the coupling between P-SV and SH waves, which is neither the case of a perfectly layered half-space (without presence of the lateral non-homogeneities) nor the case of a layered medium with two-dimensional lateral non-homogeneities. The existence of the lateral non-homogeneities in the earth medium not only affects the seismogram envelops, response spectra, and power spectra of the ground and/or underground motion to a certain extent, but also is responsible for the generation of coda waves. The extent of these effects is primarily dependent on the dominant wavelength and the intensity of the lateral non-homogeneities.

2.3. Methodology for wave propagation analysis

Among the techniques applied to analyze earthquake wave propagation, especially in a layered half-space, the discrete wave number method is perhaps most convenient and applicable, which not only takes into account all kinds of travelling waves, i.e. body waves and surface waves, but also minimizes numerical computation problems. In particular, this methodology is developed on the basis of the work of Lamb [21], Bouchon [6], Chouet [8] and Dunkin [12]. The discrete wave number technique is used to propagate waves due to the rupture of an extended seismic source through a 3-D layered half-space. With this method, it is possible to calculate the near-field and the far-field seismic ground motion at any point of a layered viscoelastic half-space, such that the spatial variability of ground motion at distances comparable to the dimensions of engineering structures can be estimated. The extent and magnitude of permanent ground deformation can also be computed, which is very important in analyzing earthquake response

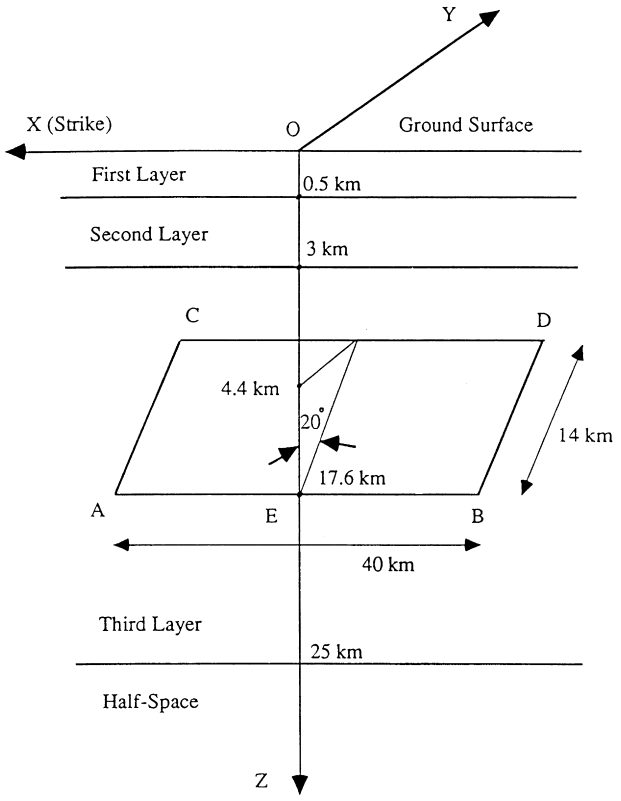

Fig. 6. Loma Prieta earthquake model.

of large scale engineering structures with relatively low natural frequencies of vibration, such as long-span bridges and base-isolated structures. In practical computation, the Green function, i.e. the response of ground motion to an effective point source associated with a double couple, may be found first using a propagator-based formalism, in which the wave radiation from the source is decoupled into P-SV and SH motions and the two problems are then solved separately. The earthquake ground motion generated by the aforementioned seismic source mechanism is then synthesized by taking into consideration the evolution of the slip and Green's functions at a certain location on the fault plane.

For the analysis of wave propagation and scattering in a layered half-space with lateral non-homogeneities, a first order perturbation approach is applied first with ease (see, e.g. [43]). Specifically, the total wave field, generated by a seismic dislocation source buried in the layered half-space, is decomposed into two wave fields. One is a mean wave field, which is a response field in a perfectly layered half-space subjected to a seismic dislocation source. This mean wave field can then be solved using the discrete wave number method. The other is a scattered wave field, which is due to the existence of lateral non-homogeneities. The effects of the non-homogeneities on the scattered wave field are equivalent to those of fictitious discontinuity sources acting on the perfectly plane boundaries in case of irregular boundaries or those of fictitious distributed body

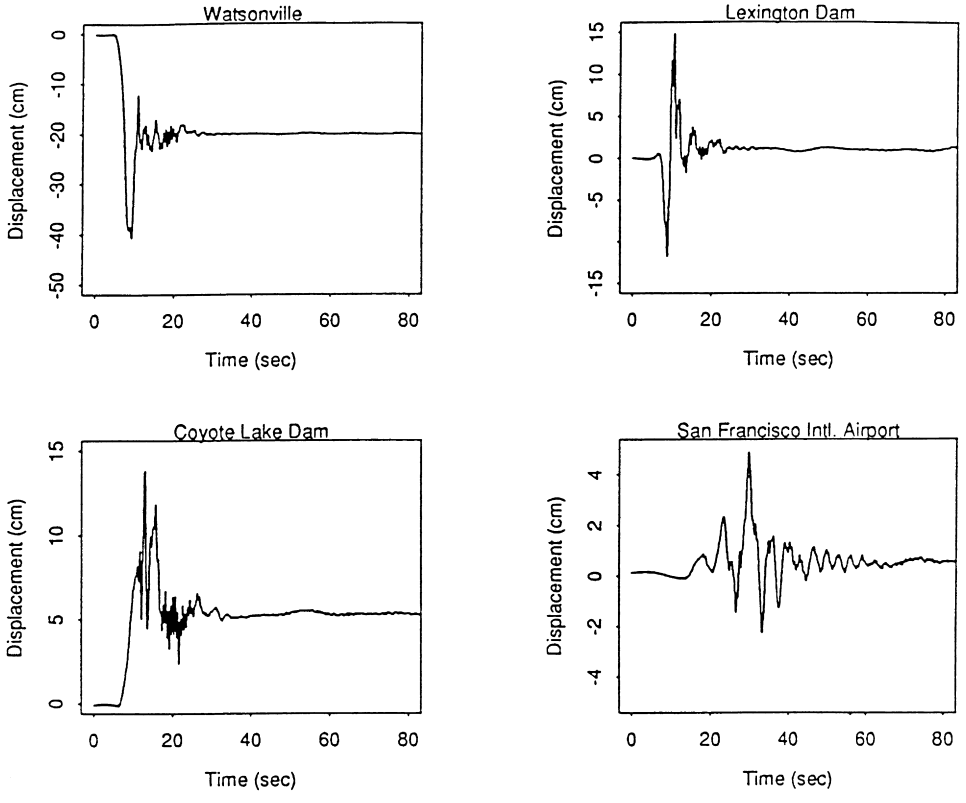

Fig. 7. Synthesized displacement time histories in the strike direction for the Loma Prieta earthquake at four observation sites [40].

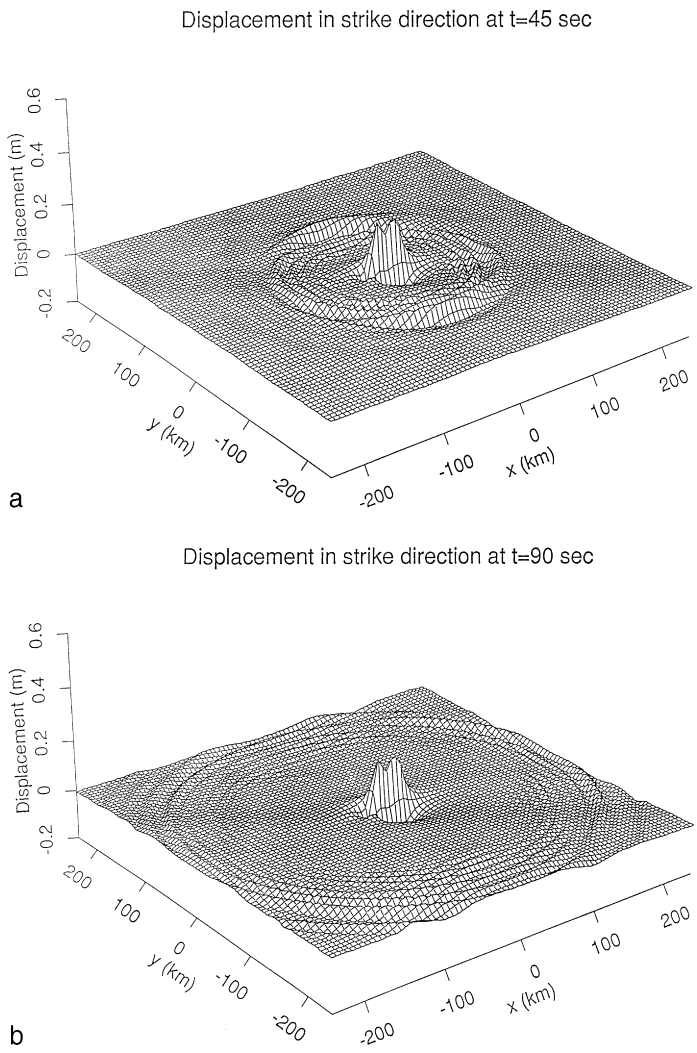

Fig. 8. (a) Synthesized displacement field in the strike direction for the Loma Prieta earthquake at 45 sec [40]. (b) Synthesized displacement field in the strike direction for the Loma Prieta earthquake at 90 sec [40].

forces that mathematically replace the lateral non-homogeneities. The intensity of the fictitious forces depends on both the mean wave response field and the lateral non-homogeneities. The solution for the scattered wave field is also obtained using the discrete wave number method.

2.4. Computer code 'seismo'

Using the aforementioned earthquake wave motion models describing the seismic source and the earth medium, and the methodology for the analysis of wave propagation and scattering, a computer code called 'SEISMO' has been developed by Deodatis, Durukal, Papageorgiou, Shinozuka, Theoharis, L. Zhang and R. Zhang. Its validity and accuracy was verified by comparing its results with corresponding results obtained by Archuleta and Hartzell [4]. The 'SEISMO' code has also been successfully used to synthesize ground motion both in the near- and the far-field for the 1968 Tokachi-Oki and the 1989 Loma Prieta earthquakes using seismologically-consistent source models (e.g. [40]). The synthesized Loma Prieta earthquake ground motion has been verified to be consistent with the actual records in terms of magnitude (intensity), wave form (frequency content) and time duration.

The 'SEISMO' computer code needs as input information describing the earth medium and the seismic source and generates as output the synthesized ground motion time histories at the near field and the far field, including permanent ground deformation. Time histories can be provided either at prescribed observation sites, or at a large rectangular grid of points over a large area on the ground surface.

2.5. Numerical examples

Three numerical examples of synthesized ground motion are presented in the following to illustrate the use of the aforementioned earthquake wave motion models and the 'SEISMO' computer code.

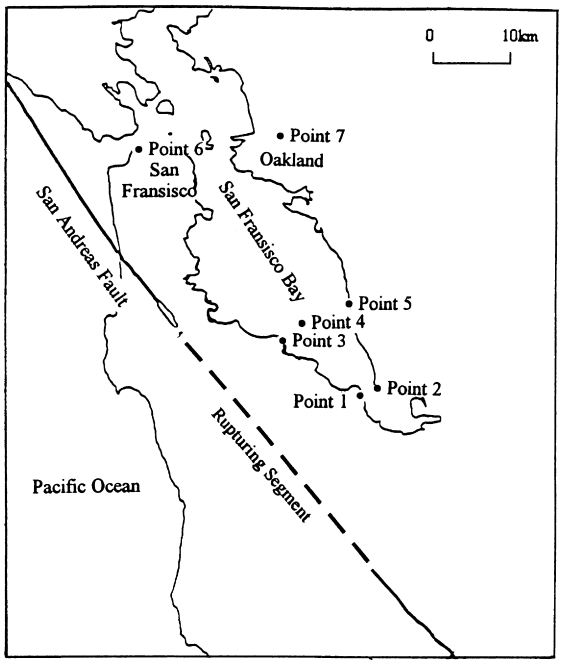

Fig. 9. The 40 km long rupturing segment of the San Andreas fault and the location of the seven points [11].

Table 1
Desription of the cases considered in the simulations [10]

	Slip type	Rupture pattern	Dislocation function
Case 1	Strike		Ramp function
Case 2	Strike slip		Barrier model (as described in text)
Case 3	Strike slip		Barrier model (as described in text)
Case 4	Strike slip		Barrier model (as described in text)
Case 5	Strike slip-Dip slip		Barrier model (as described in text)
Case 6	Strike slip-Dip slip		Barrier model (as described in text)
Case 7	Strike slip-Dip slip		Barrier model (as described in text)

2.5.1. Loma prieta earthquake ground motion

The 1989 Loma Prieta earthquake ground motion was synthesized by Zhang and Deodatis [40] using the seismologically-consistent source model suggested by Zeng [35,36] and a layered half-space earth model (see Fig. 6). The final slip distribution shown in Fig. 4 was used in this study. Fig. 7 displays the ground displacement time histories at selected observation sites, while Figs. 8a and b present the synthesized wave motion at a dense grid of observer locations at selected time instants. The generation and propagation of different kinds of seismic waves, the spatial and temporal variability of ground motion, as well as the development of the permanent (static) ground deformation, can be examined by carefully studying the plots in Figs. 7 and 8.

2.5.2. Loma prieta-type earthquake ground motion

For this scenario earthquake presented by Deodatis et al. [10] a portion of the San Andreas fault close to the San Francisco Bay area is assumed to rupture, as shown in Fig. 9. Seven different cases of radial rupture patterns are considered. These seven cases, displayed graphically in Table 1, differ in the location of the hypocenter. Displacement traces on the ground surface are computed at the seven locations indicated in Fig. 9 using the barrier model with irregular boundaries depicted in Fig. 10. The first five points correspond to the abutments of two bridges in the area, point 6 is in San Francisco, and point 7 is in Oakland. Fig. 11 displays the traces of particle motions on the horizontal plane at points 3, 4 and 5. These results are very useful for the sensitivity analysis of structural response characteristics due to spatial variation of ground motion.

2.5.3. Effects of lateral non-homogeneities on ground motion

While the previous two examples use a perfectly layered half-space as the earth medium model, the effects of lateral non-homogeneities of the earth medium are examined in this one. In particular, the earth medium is modeled as two layers over a half-space with the top layer properties being laterally non-homogeneous. In other words, the wave speeds and density of the top layer are functions of lateral coordinates. For comparison, two kinds of the common factor $a(x,y)$, characterizing the perturbed parts of P and S wave speeds and density of the top layer, are shown in Fig. 12. The vertical ground accelerations due to a point source (which is done for simplicity and demonstration; it is straightforward to extend the case of the point source to that of the extended source) at selected observation sites with and without the presence of lateral non-homogeneities are depicted in Fig. 12. It can be seen from Fig. 12 that the effects of ‘smooth’ (longer dominant wavelength) lateral non-homogeneities on the ground motion are primarily on the variation in peak acceleration, while the effects of ‘rough’ (shorter dominant wavelength) lateral non-homogeneities on the ground motion are primarily on the

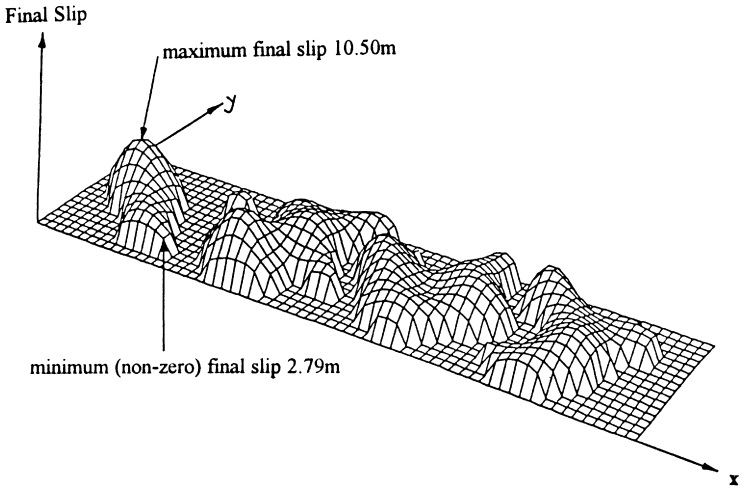

Fig. 10. Distribution and amount of final slip over the fault plane using a barrier model with irregular boundaries (M = 7) [11].

broadening of the seismogram envelops. These phenomena are consistent with what Aki [3] and Sato [29] observed in their relatively simple models. Fig. 13 presents the perturbed depth of the irregular interface between the top layer and the second layer and its effect on the ground acceleration. The results are similar to those of laterally non-homogeneous medium properties shown in Fig. 12.

2.6. Near-field motion effects on long-period structures

The establishment of sophisticated earthquake motion models, as aforementioned, is fundamental and useful to understand the occurrence of an earthquake from the physics point of view. However, it may be questionable for its practical usefulness from the engineering point of view if the earthquake ground motion records can be obtained. However, recent large earthquakes, especially the Northridge and the Kobe earthquakes, have provided an extremely good lesson to both seismologists and engineers. Firstly, the nature of near-field ground motion strongly depends on seismic source characteristics such as location, directivity and pattern of shear dislocation. Consequently, the study of the effect of near-field earthquakes on structures is much more difficult and complex than for far-field earthquakes. Secondly, the existing records associated with the near field quite often distort the nature of the shaking, especially for low-frequency components, due to the high-pass filtering in processing the data obtained from seismometers of earlier vintage. The low-frequency ground motion is believed to be capable of causing significantly high percentage of story drift in case of high-rise buildings or very large pad displacement in case of base-isolated buildings [14,16]. Since the occurrence of large earthquakes in urban areas is highly likely in California (e.g. the 30-year probability for the San Francisco Bay area to be subjected to an earthquake with a magnitude being 7.0 or larger has been estimated to be about 67%), it becomes important to study the nature of the low-frequency components of the near-field earthquake ground motion and its effect on long-period structures.

At this juncture, the aforementioned earthquake motion model plays an important role in capturing the nature of near-field ground motion. Due to the high-pass filtering in processing the data obtained from the seismometers of earlier vintage, the observed ground motion cannot always be adequately used to examine its effect on flexible structures. Recently, Zhang and Shinozuka [44] applied the aforementioned earthquake motion model and SEISMO to show the extent of the underestimation of the response spectra with the use of observed ground motion, and to study the effects of source information such as rupture pattern, slip distribution as well as directivity of the fault on the response spectra.

Specifically, the Loma Prieta earthquake is used as an example again, in which the simulated and observed ground motion at selected observation sites are compared and the corresponding response spectra to both simulated and observed ground motion are then calculated. Consequently, the low-frequency near-field motion effects on long-period structures can be analyzed.

The near-field ground motion is first simulated, which consists of two parts. The low-frequency part (up to 1 Hz) is synthesized using computer code SEISMO. The high-frequency part is obtained by modifying real earthquake records by deleting the corresponding low-frequency part from the recorded data and adjusting peak magnitude on the basis of the relative distance away from the observation sites. The reasons why the synthetics and filtered recorded data are combined to form the simulated ground motion are detailed as follows. (1) Many studies indicated that the synthetics of the ground motion by using theoretical models can successfully predict the ground motion in the low-frequency range (usually less than 1.5 Hz). However, the synthetics of higher frequency motion are

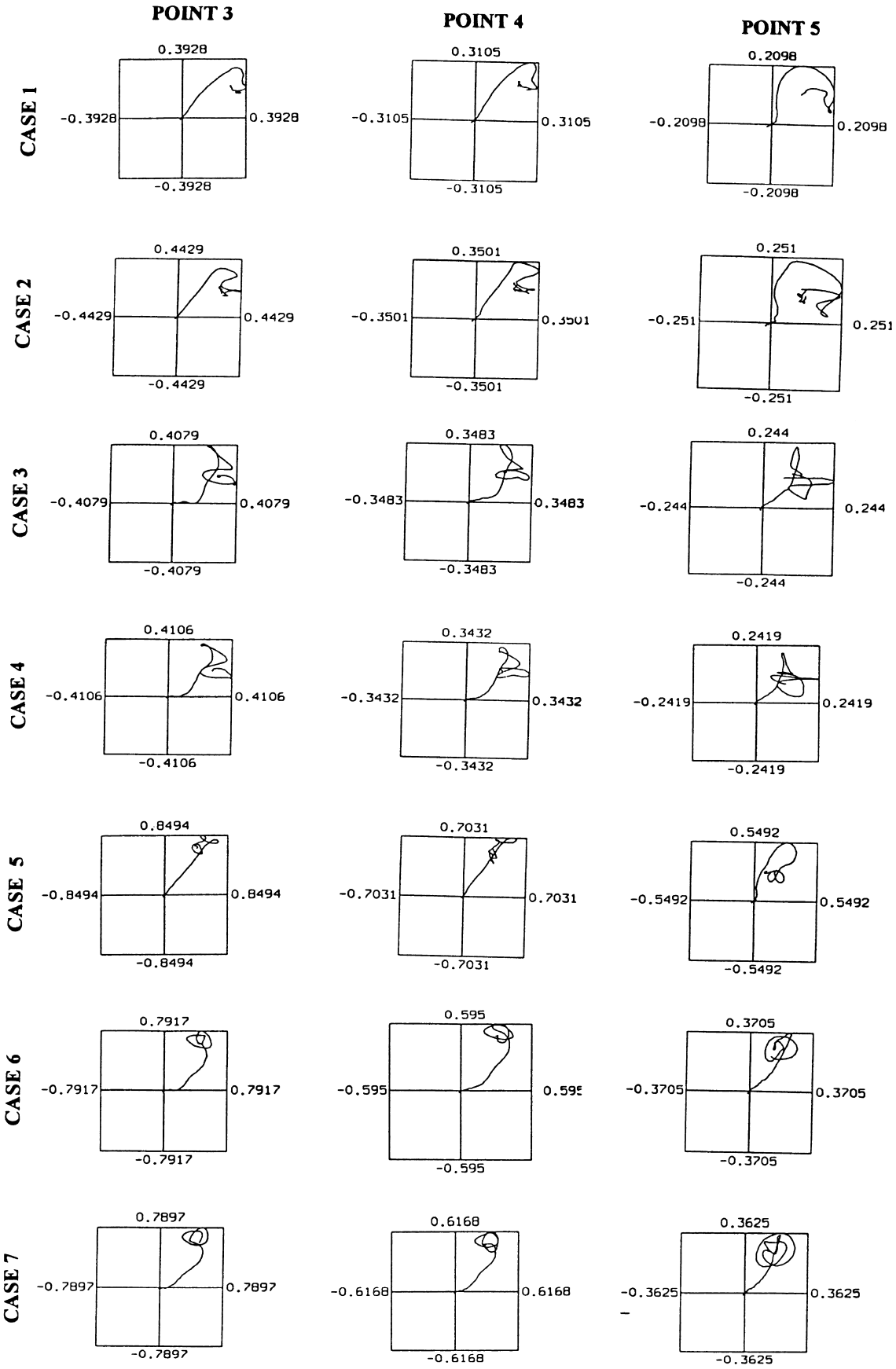

Fig. 11. Traces of particle motions on the horizontal plane at points 3, 4 and 5 [11].

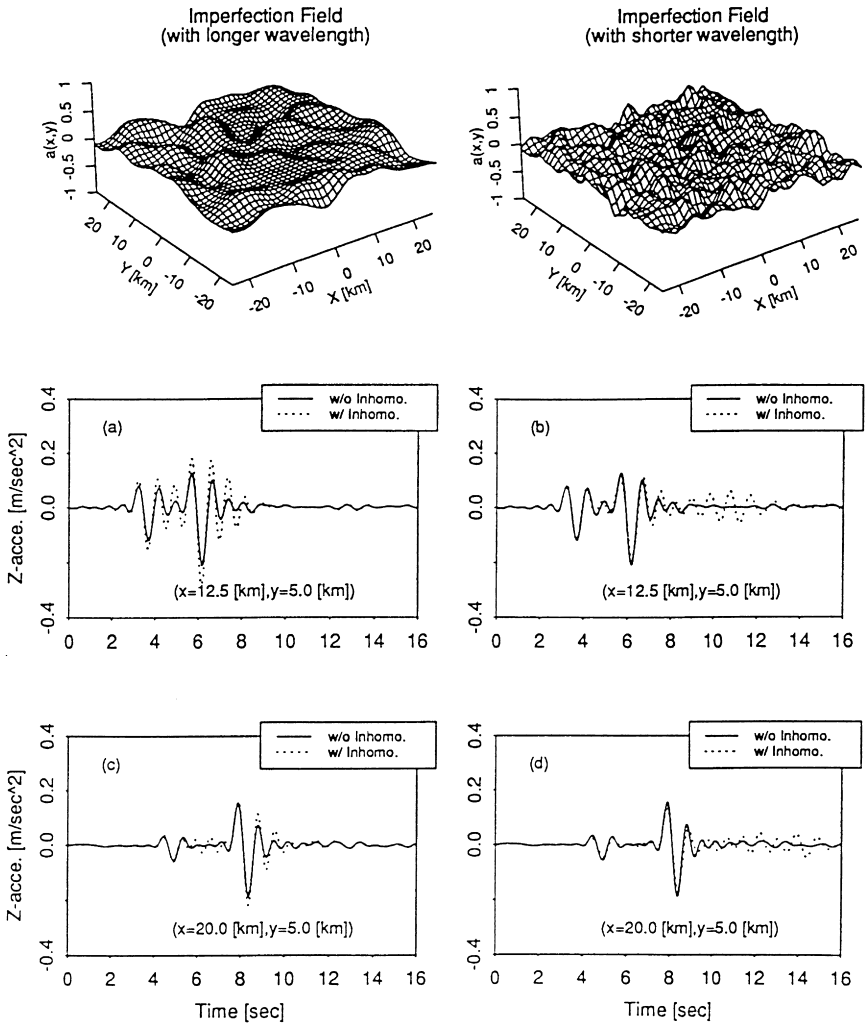

Fig. 12. Simulated common factor $a(x,y)$, characterizing the perturbed medium properties, and its effect on ground acceleration time histories [42].

either time-consuming using the theoretical models or not as good as the prediction of low-frequency motion. (2) The existing records particularly at near field quite often distort the nature of the shaking, especially for low-frequency motion. For example, some accelerometers do not record very low frequency components (e.g. less than 0.1 Hz). In addition, the relatively low frequency components (e.g. less than 0.3 Hz) of the recorded data are underestimated [19]. (3) As far as the long-period structures are concerned, the high-frequency motion is not as important as the low-frequency, especially beyond the frequency larger than 1 Hz.

Fig. 14 shows the simulated and observed ground motion at Santa Cruz (16 km away from the epicenter), while Fig. 15 presents the corresponding response spectra.

As can be seen from Figs. 14 and 15, richer low-frequency content of ground motion can be observed in the simulation rather than in the recorded data, resulting in larger acceleration responses for moderate to long periods (1 to 6 sec). This implies that the use of recorded data underestimates the response of structures having moderate to long periods.

3. Statistical estimation of strong ground motion

The spatial variation of earthquake ground motion has non-negligible effects on elongated structures such as bridges, underground pipelines, etc. While the ground motion is non-stationary in time and non-homogeneous in space, the essential feature of the spatial and temporal variation is usually captured by idealizing it as a stationary and homogeneous function of time and space, at least within an appropriate time-space window (composed of a space window and a time window), which may be seen schematically in Fig. 16. Only with this idealization is it possible to examine the effects of spatial variation of ground motion on the structural response by taking advantage of such quantities as the frequency-wave number (F-K) spectrum, cross-spectral density function matrix, coherence function and the like. Given the F-K spectrum, the corresponding seismic ground motion can be numerically simulated [11,30,31] which can be used for carrying out the time-space domain structural analysis, particularly non-linear structural analysis.

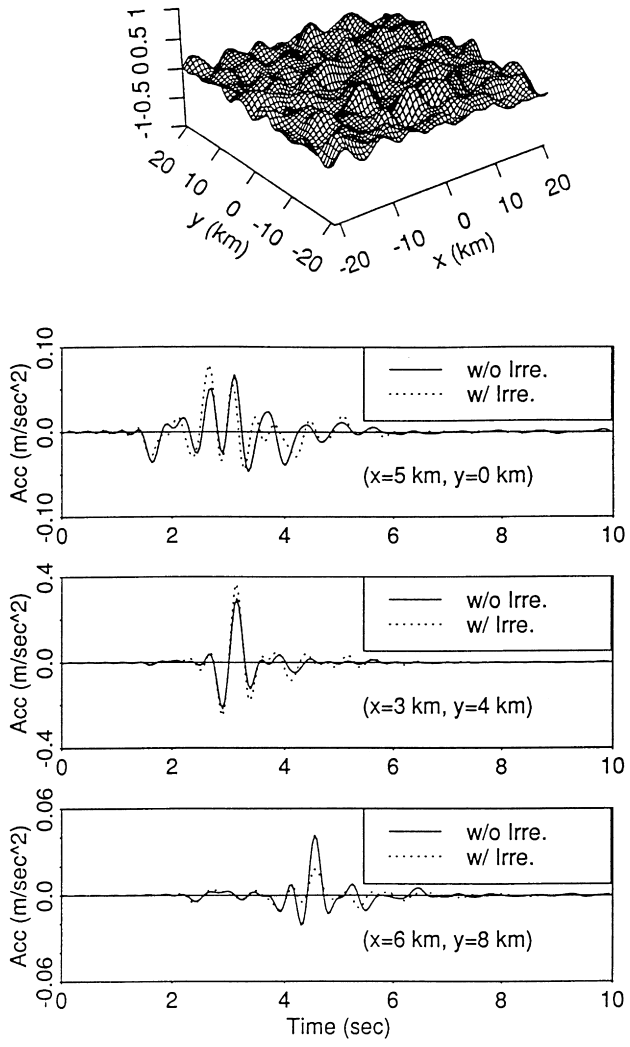

Fig. 13. Simulated perturbed depth of the irregular interface $a(x,y)$ and its effect on ground acceleration time histories [40].

The spatial and temporal statistics of ground motion are usually estimated with the aid of many earthquake records. In particular, Bolt et al. [5], Abrahamson and Bolt [1], Loh and Yeh [27] and Toksoz et al. [34] used earthquake records from relatively small areas, notably the data obtained from SMART 1 array in Lotung, Taiwan, to estimate the F-K spectrum, while Loh et al. [26], Loh [24], Harichandran and Vanmarcke [15], Zerva et al. [37], Abrahamson et al. [2], Katayama [20] and Ellis and Cakmak [13] estimated either frequency-dependent spatial correlation functions or coherency functions at differing levels of analytical sophistication. The approach proposed and used by the aforementioned researchers can also be served for other earthquakes such as the Loma Prieta earthquake to find the corresponding statistics. However, the obtained statistics are, strictly speaking, valid and useful only in the area where many earthquake records are available. Consequently, the engineering applications of these strong motion statistics are used only in restricted areas unless some pertinent assumptions are made appropriately.

On the other hand, in the last two decades, seismologists and engineers have focused their attentions on establishing theoretical models for earthquake wave motion in such a way that the synthesized ground motion using the model will be consistent, in a seismological sense (with respect to peak value, frequency content, and time duration of earthquake motion), with the real earthquake ground motion at several locations where records are available. The model so established is thus reliable and the synthesized ground motion can be regarded as a 'true' earthquake in the seismological sense. Such an endeavor will recover the ground motion of the modelled earthquake where the recorded data are not available.

While the synthesized seismologically-consistent ground motion is useful for better understanding of the ground motion properties such as the seismic wave propagation, it has also provided a theoretical basis for the study of the statistical properties of ground motion including spatial variability. Unfortunately, such an important engineering application has not yet received full attention.

Recently, Zhang [39] proposed a computational procedure to estimate spatial and temporal statistics of ground motion in a time-space window on the basis of a synthesized ground motion using the theoretical earthquake wave motion model that has been detailed in the previous section. Since the synthesized ground motion can be computed at any location over the ground surface, the statistics of ground motion can thus be estimated wherever they are needed regardless of whether the recorded data are available or not. This is the unique merit of the proposed procedure that the standard estimation does not have. In addition, since many theoretical models have been established by seismologists for real earthquakes such as Loma Prieta, Northridge and Kobe earthquakes, the statistical analysis for the effects of spatial variation of these earthquake ground motions on the structures can thus be carried out with the aid of the proposed methodology.

3.1. Proposed estimation approach in a time-space window

In the present study, the ground motion $f(x,y,t)$ is expressed in terms of an infinite number of plane waves having the integral representation satisfying the specified boundary conditions, and originating from the prescribed seismic source. This procedure is consistent with the discretized wave number solution, and used by many other researchers (e.g. [33]). The solution takes the following form:

$$f(x,y,t) = \int_{-\infty}^{\infty}\int_{-\infty}^{\infty}\int_{-\infty}^{\infty} \tilde{f}(\kappa_x,\kappa_y,\omega)\exp[i\kappa_x x + i\kappa_y y + i\omega t]d\kappa_x d\kappa_y d\omega \quad (13)$$

where $f(x,y,t)$ is the ground motion of displacement, velocity, or acceleration, and $\tilde{f}(\kappa_x,\kappa_y,\omega)$ is the Fourier transform of ground motion. In this procedure, $\tilde{f}$ may be found first by

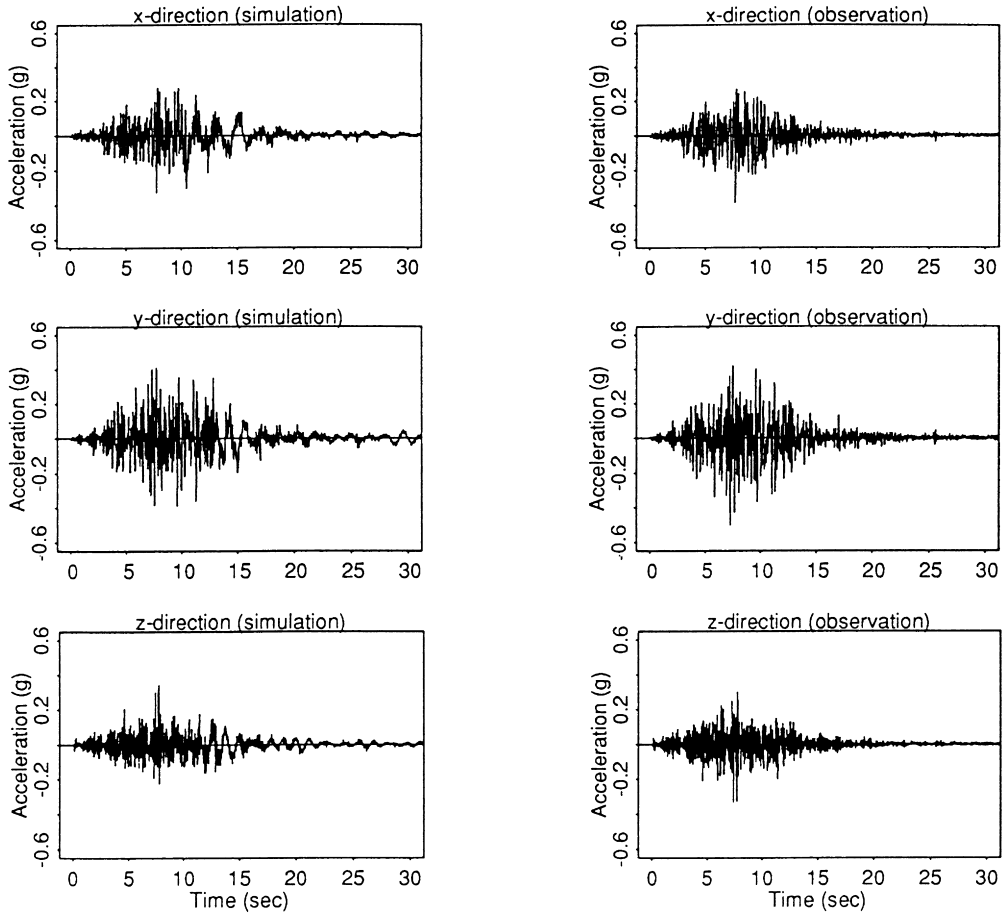

Fig. 14. Simulated and recorded earthquake ground acceleration at Santa Cruz [44].

using the methodology described in Section 2.3 and the three-fold Fourier transform is then performed to obtain the ground motion in the time-space domain. As asserted earlier, the ground motion $f(x,y,t)$ is neither homogeneous in space (x,y) nor stationary in time t. However, a time-space window may be properly selected so that the corresponding ground motion in the window can be considered as both a homogeneous and stationary function of (x,y,t) in approximation, as shown in Fig. 16.

Considering a time-space window centered at (x_0,y_0,t_0) or equivalently (r_0,θ_0,t_0) with window lengths being (X_w,Y_w,T_w), as shown in Fig. 16, the corresponding ground motion in the window f_W may have the following integral representation:

$$f_W(x,y,t) = \int_{-\infty}^{\infty}\int_{-\infty}^{\infty}\int_{-\infty}^{\infty} \tilde{f}_W(\kappa_x,\kappa_y,\omega)\exp[i\kappa_x x + i\kappa_y y + i\omega t]d\kappa_x d\kappa_y d\omega. \tag{14}$$

Noticing the following fact

$$f_W(x,y,t) = f(x,y,t); (x,y,t) \in \textit{ the window}. \tag{15}$$

One may find the following relationship between $\tilde{f}_W$ and $\tilde{f}$:

$$\tilde{f}_W(\kappa_x,\kappa_y,\omega) = \int_{-\infty}^{\infty}\int_{-\infty}^{\infty}\int_{-\infty}^{\infty} \tilde{f}(\kappa_x',\kappa_y',\omega')w(\kappa_x' - \kappa_x;x_0,X_W)w(\kappa_y' - \kappa_y;y_0,Y_W)w(\omega' - \omega;t_0,T_W)d\kappa_x' d\kappa_y' d\omega' \tag{16}$$

where window function $w(\Delta;c,W) = sin(\Delta W/2)exp[i\Delta c]/\pi/\Delta$. It can be seen clearly from Eq. (16) that the representation of $\tilde{f}_W$ is a three-fold convolution of $\tilde{f}$ involving three window functions w. However, the three-fold convolution can be actually carried out quickly in numerical computation, since w will die down quickly as Δ increases. In the case of T_W, X_W, and Y_W being very large, the selected window is actually equivalent to the original entire time-space domain, and Eq. (16) will thus result in $\tilde{f}_w \simeq \tilde{f}$.

In many engineering applications, (T_W,X_W,Y_W) can be appropriately selected so that the ground motion can be assumed to be both stationary and homogeneous within this window (e.g. Fig. 16). Further, it is usually assumed that ground motion in the window is ergodic in both time t and space (x,y). Therefore, the correlation function of the

ground motion in the window can be found as

$$R_{f_w}(\xi_x, \xi_y, \tau) = \frac{1}{T_W X_W Y_W} \int_{t_0-T_W'/2}^{t_0+T_W'/2} \int_{y_0-Y_W'/2}^{y_0+Y_W'/2} \int_{x_0-X_W'/2}^{x_0+X_W'/2} f_W(x, y, t) f_W(x + \xi_x, y + \xi_y, t + \tau) dx dy dt \tag{17}$$

where ξ_x and ξ_y are respectively the separation distances in the x- and y-directions, τ is the time lag, $X_W' = X_W - 2|\xi_x|$, $Y_W' = Y_W - 2|\xi_y|$ and $T_W' = T_W - 2|\tau|$.

Substituting the integral representation of f_W into Eq. (17) and using the three-dimensional version of the Wiener-Khintchine transform theorem, one may obtain the F-K spectrum P_{f_w} of the ground motion in the window as

$$P_{f_w}(\kappa_x, \kappa_y, \omega) = \frac{(2\pi)^3}{T_W X_W Y_W} \int_{-\infty}^{\infty} \int_{-\infty}^{\infty} \int_{-\infty}^{\infty} \tilde{f}_W * (\kappa_x', \kappa_y', \omega') \tilde{f}_W(\kappa_x, \kappa_y, \omega) w(\kappa_x - \kappa_x'; x_0, X_W') w(\kappa_y - \kappa_y'; y_0, Y_W') w(\omega - \omega'; t_0, T_W') d\kappa_x' d\kappa_y' d\omega' \tag{18}$$

where the asterisk stands for the complex conjugate. As indicated before, the three-fold convolution can be carried out quickly in numerical computation as long as the window lengths selected are not too short. When the window lengths, (T_W, X_W, Y_W), are selected to be very long, the window function may be approximated as a Delta function, resulting in the F-K spectrum given by

$$P_{f_w}(\kappa_x, \kappa_y, \omega) \simeq (2\pi)^3 |\tilde{f}_W(\kappa_x, \kappa_y, \omega)|^2 / (T_W X_W Y_W) \tag{19}$$

which is consistent with common practice in general and with the approximation used by Theoharis [33] in particular. However, the assumption of stationarity and homogeneity of ground motion for a much larger window may not be appropriate for the present purpose.

An F-K spectrum essentially contains all the information of the temporal and spatial statistics of ground motion in the selected window. Other statistics of ground motion can be obtained directly from the F-K spectrum. For example, the cross-spectral density function can be obtained by

$$C_{f_w}(\xi_x, \xi_y, \omega) = \int_{-\infty}^{\infty} \int_{-\infty}^{\infty} P_{f_w}(\kappa_x, \kappa_y, \omega) \exp[i\kappa_x \xi_x + i\kappa_y \xi_y] d\kappa_x d\kappa_y. \tag{20}$$

The power spectral density function is obtained from the cross-spectral density function, i.e.

$$S_{f_w}(\omega) = C_{f_w}(\xi_x = 0, \xi_y = 0, \omega) = \int_{-\infty}^{\infty} \int_{-\infty}^{\infty} P_{f_w}(\kappa_x, \kappa_y, \omega) d\kappa_x d\kappa_y. \tag{21}$$

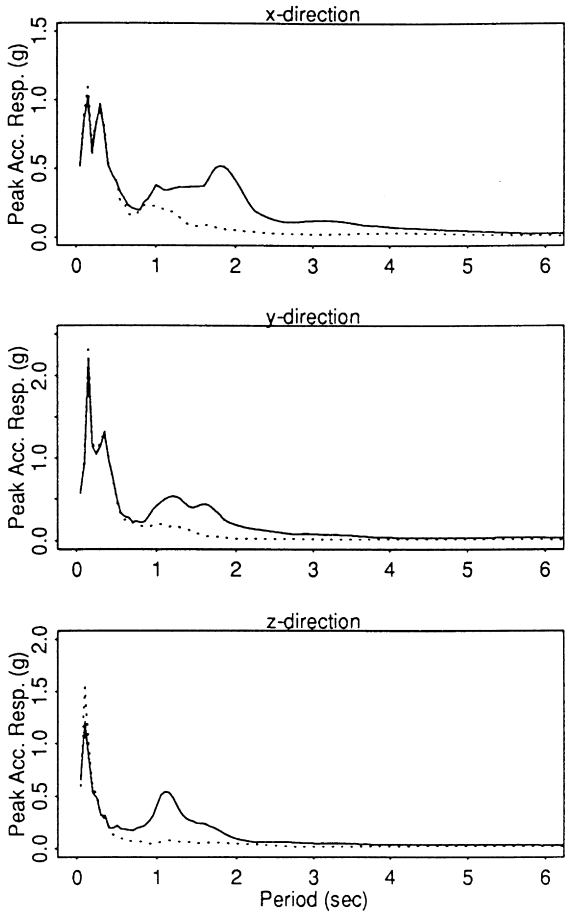

Fig. 15. Acceleration response spectra with 5% damping ratio at Santa Cruz (solid line is associated with simulated motion and dotted line with recorded motion) [44].

Finally, the frequency-dependent coherence function is obtained as

$$\gamma_{f_w}(\xi_x, \xi_y, \omega) = |C_{f_w}(\xi_x, \xi_y, \omega)| / S_{f_w}(\omega). \tag{22}$$

Two numerical examples are presented below for illustration of the statistical estimation of strong ground motion.

3.2. Verification: statistics of ground motion time history

The first example is designated as a special case of the study, which is the estimation of the power spectral density (PSD) function of the Loma Prieta earthquake ground motion at the given observation site.

The ground acceleration is shown at the top of Fig. 17. Apparently, the ground motion in Fig. 17 is non-stationary. Nevertheless, it can be considered as a piece-wise stationary process. In particular, the ground motion is assumed as stationary within each of three windows centered respectively at time $t_0 = 5$, 14 and 30 sec with all window lengths being $T_W = 8$ sec. Furthermore, the ground motion in each of the three windows is considered to be ergodic.

Fig. 17 also shows a comparison between the estimate of the PSD function using the proposed approach [39] and that

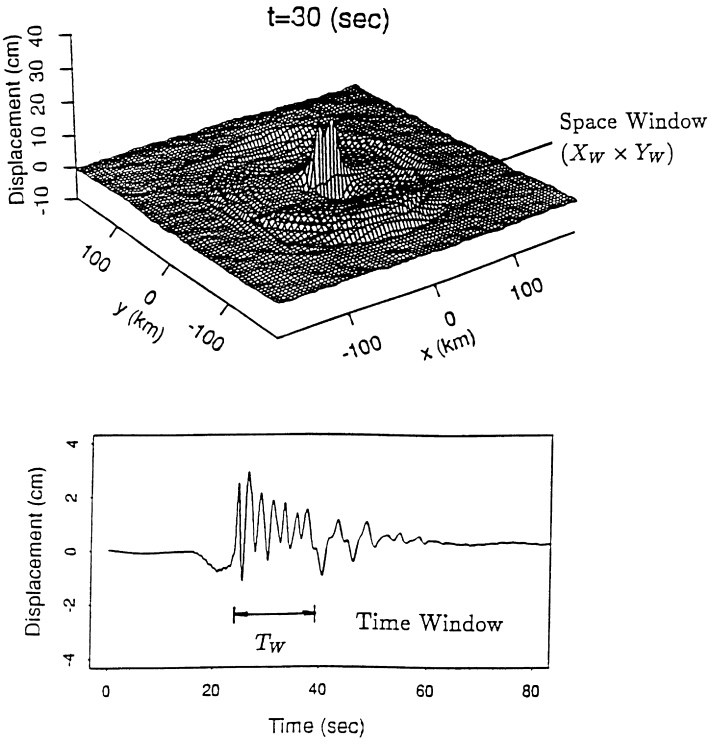

Fig. 16. Schematic of a time and a space window selected for a strong ground motion event [39].

using the method proposed by Liu and Jhaveri [23] and Liu [22]. Comparing plots in Fig. 17, one can immediately see that the estimates of the PSD function using the proposed and Liu's approaches are basically consistent with respect to frequency content and magnitude (intensity), confirming the validity of the proposed methodology.

3.3. Applications: statistics of ground motion field

As the second example, the statistics of the Loma Prieta earthquake ground motion in a local area (a time-space window) are calculated and discussed.

Although the statistics of ground motion in any given time-space window may be obtained using the proposed method, only the strong ground motion that is related to a certain time window for a given space window is useful for engineering applications. For example, the ground velocity and acceleration are zero when all the seismic waves have not reached or have passed over a given space window in some time windows, which is obviously useless information to practical engineering. This may be confirmed in Fig. 16. Therefore, it is important to select properly a time window for a given space window so that the statistical characteristics of the strong ground motion in the time-space window can be captured.

It is well-known that earthquake ground motion consists of various seismic waves including body waves (P and S waves and their combination) and surface waves (e.g. Rayleigh and Love waves). The primary energy of seismic waves is carried by the S and surface waves. Therefore, the center of a time window for the strong ground motion in a given space window should be located no earlier than the time the first S wave signal propagates directly from the hypocenter (coordinate origin) to the space window center. On the other hand, the center of a time window should not be located too much later than the time the last S wave signal propagates directly from the source to the given space window. Otherwise, most of S and possibly surface waves pass over the given space window. For more information about the appropriate selection of a timespace window, the reader is referred to Zhang [39]. According to these guidelines, a window is selected for this numerical example, which is centered at ($t_0 = 20$ sec, $x_0 = 17$ km, $y_0 = 10$ km) with window lengths being ($T_W = 15$ sec, $X_W = Y_W = 15$ km). The F-K spectra and coherence functions of the ground acceleration in the selected window at $\omega = 5$, 10, 20 and 30 rad/sec are computed, and displayed respectively in Fig. 18Fig. 19. As seen in Fig. 18, the maximum values of the F-K spectra are relatively small at both low ($\omega = 5$ rad/sec) and high ($\omega = 30$ rad/sec) frequencies, compared with those at the middle frequency range ($\omega = 10$ and 20 rad/sec), which indicates that the dominant energy carried by the acceleration lies in the window from $\omega = 10$ to 20 rad/sec. Fig. 19 shows that as the separation distance increases, the coherence decays exponentially in an oscillatory fashion at a given frequency, and more quickly so at high frequencies rather than at low frequencies, as expected. The coherence characteristics observed in the present numerical examples are basically consistent with those obtained using actual earthquake records observed at the SMART 1 array, as indicated by Loh and Yeh [27] and Loh [25].

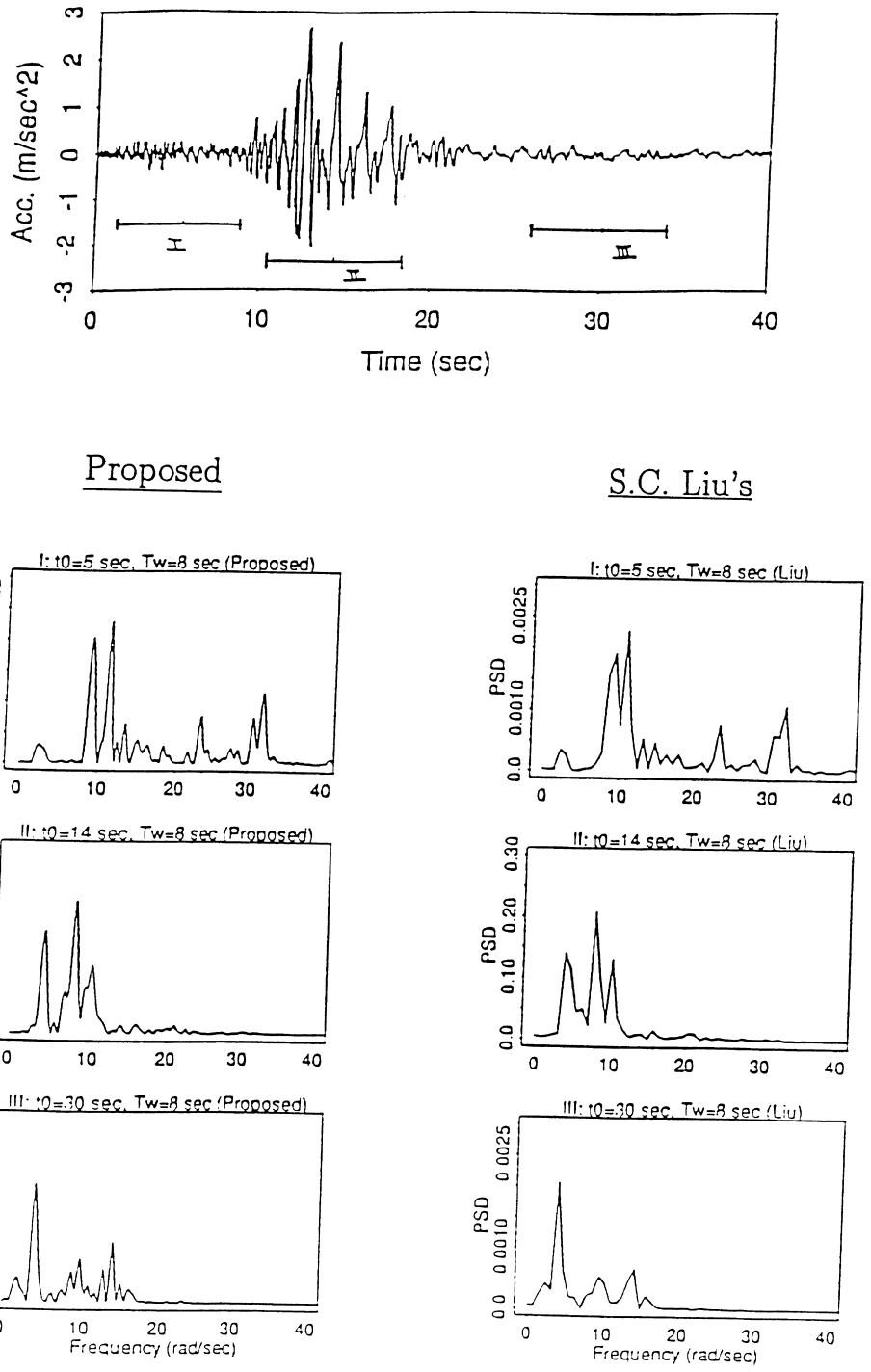

Fig. 17. Loma Prieta ground acceleration at a given location and comparison of proposed and Liu's estimates of the power spectral density function at selected windows [39].

4. Conclusions and remarks

In summary, this paper covers two earthquake-wave-motion-related topics. The first one related to earthquake wave motion modeling examines uncertainties in the modeling of the earth medium and the seismic source. The second deals with the estimation of statistical characteristics of synthesized strong ground motion such as the frequency-wave number spectrum and the coherence function, which are used in simulating spatially-correlated earthquake ground motions.

Among the numerous potential applications of synthesized and simulated seismic ground motion, the following ones are mentioned here: inundation by tsunamis, liquefaction

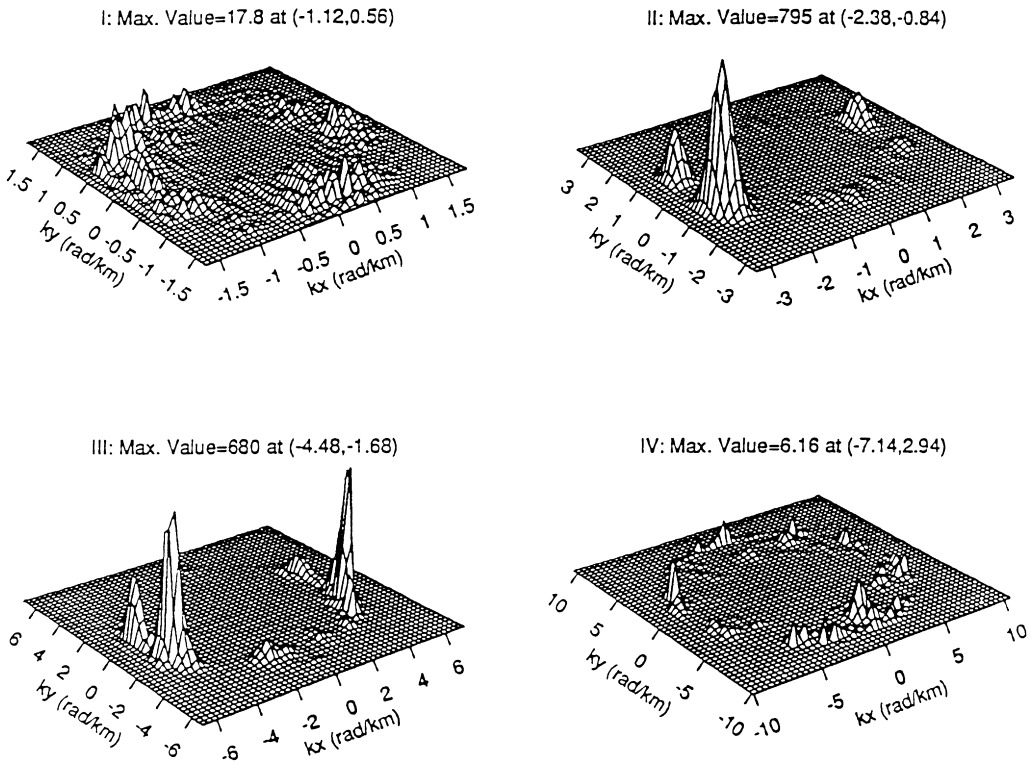

Fig. 18. F-K spectra of the Loma Prieta earthquake ground acceleration in the strike direction at frequncies of 5, 10, 20 and 30 rad/sec respectively for plots I, II, III and IV [39].

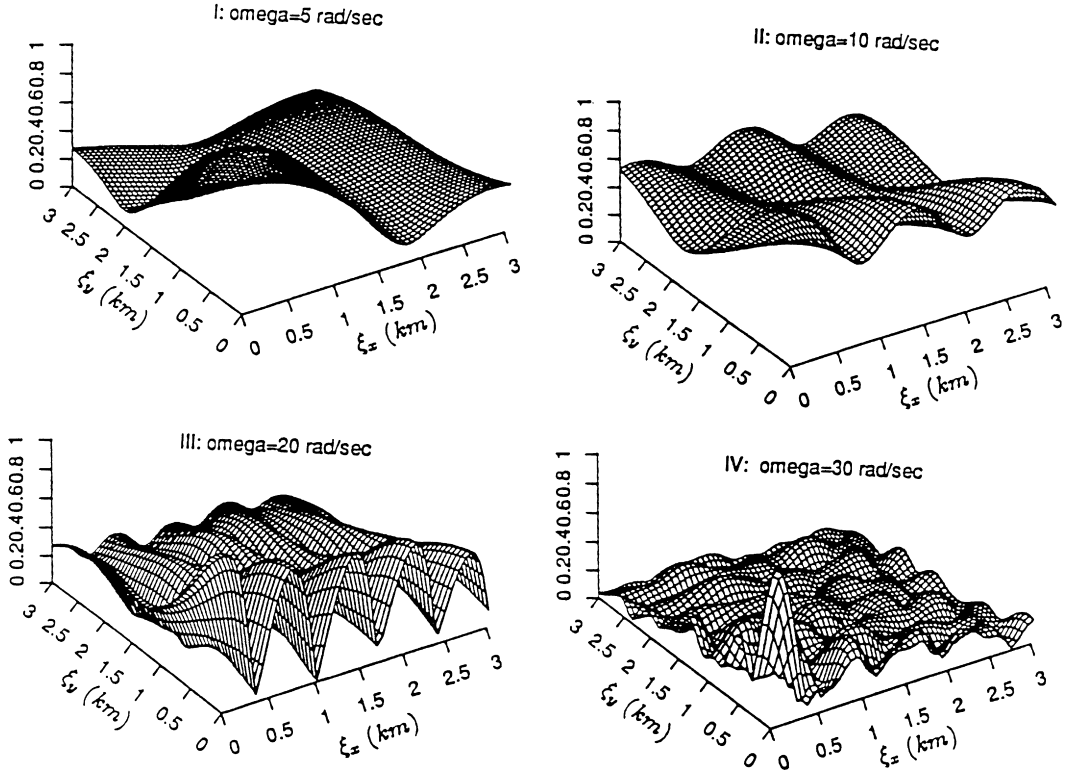

Fig. 19. Coherence functions of the Loma Prieta earthquake ground acceleration in the strike direction at frequencies of 5, 10, 20 and 30 rad/sec respectively for plots I, II, III and IV [39].

phenomena and their effect on foundation and underground facilities, structural reliability, vertical component motion effects on earthquake-resistant structural design.

Acknowledgements

This work was supported by the National Science Foundation under Grants # BCS9257900 and # BCS-9523092 with Dr. Clifford J. Astill as Program Director, Grant # 94-3302A, # 96-12127 and #98-96070 with Dr. S.C. Liu as Program Director, by the Federal Highway Administration through the National Center for Earthquake Engineering Research under Contract # DTFH61-92-C-00106, by the U.S. Geological Survey with Contract # 98CRSA1077, and by Colorado School of Mines under Grant # CSM2-30131.

References

[1] Abrahamson N, Bolt BA. The spatial variation of the phasing of seismic strong ground motion. Bulletin of the Seismological Society of America 1985;75(5):1247–1264.
[2] Abrahamson et al. (1991). Author please provide details.
[3] Aki K. Original of coda waves: source, attenuation, and scattering effects. Journal of Geophysical Research 1975;80:3322–3342.
[4] Archuleta RJ, Hartzell S. Effects of fault finiteness on near-source ground motion. Bulletin of the Seismological Society of America 1981;71(4):939–957.
[5] Bolt BA, Tsai YB, Yeh K, Hsu MK. Spatial coherency of shear waves from the Lotung, Taiwan large-scale seismic test. Earthquake Engineering and Structural Dynamics 1982;10(4):561–573.
[6] Bouchon M. Discrete wave number representation of elastic wave fields in three-dimensional space. Journal of Geophysical Research 1979;84(B7):3609–3614.
[7] Caviglia G, Morro A. Inhomogeneous waves in solids and fluids. Singapore: World Scientific, 1992.
[8] Chouet B. Representation of an extended seismic source in a propagator-based formalism. Bulletin of the Seismological Society of America 1987;77(1):14–27.
[9] Chu L, Askar A, Cakmak S. Earthquake waves in a random medium. International Journal for Numerical and Analytical Methods in Geomechanics 1981;5:79–96.
[10] Deodatis G, Durukal E, Papageorgiou G, Shinozuka M. Synthesis of ground motions of a Loma Prieta-type earthquake in the vicinity of the San Francisco metropolitan area. In Proceedings of the 11th World Conference on Earthquake Engineering, Acapulco, Mexico, 23–28 June 1996, on CD-ROM.
[11] Deodatis G, Shinozuka M. Simulation of seismic ground motion using stochastic waves. J Engineering Mechanics 1989;115(12):2723–2737.
[12] Dunkin JW. Computation of modal solutions in layered, elastic media at high frequencies. Bulletin of the Seismological Society of America 1965;55(2):335–358.
[13] Ellis GW, Cakmak AS. Effects of spatial variability on ARMA modeling of ground motion. Structural Safety 1991;10(1–3):181–191.
[14] Hall JF, Heaton TH, Halling MW, Wald DJ. Near-source ground motion and its effects on flexible buildings. Earthquake Spectra 1995;11(4):569–605.
[15] Harichandran RS, Vanmarcke EH. Stochastic variation of earthquake ground motion in space and time. Journal of Engineering Mechanics 1986;112(2):154–174.
[16] Heaton TH, Hall JF, Wald DJ, Halling MW. Response of high-rise and base-isolated buildings to a hypothetical M_W 7.0 blind thrust earthquake. Science 1995;267:206–211.
[17] Reference deleted.
[18] Ishimaru A. Wave propagation and scattering in random media, vol. 1 and 2. New York: Academic, 1978.
[19] Iwan W, Chen X. Important near-field ground motion data from the Landers earthquake. Proceedings of 10th European Conference on Earthquake Engineering, Vienna, Austria, 1995.
[20] Katayama T. Use of dense array data in the determination of engineering properties of strong motions. Structural Safety 1991;10:219–233.
[21] Lamb H. On the propagation tremors at the surface of an elastic solid. Philosophical Transactions of the Royal Society of London 1904;203:1–42.
[22] Liu SC. Evolutionary power spectral density of strong-motion earthquakes. Bulletin of the Seismological Society of America 1970;60(3):891–900.
[23] Liu SC, Jhaveri DP. Spectral and correlation analysis of ground-motion acceleration. Bulletin of the Seismological Society of America 1969;59(4):1517–1534.
[24] Loh CH. Analysis of spatial variation of seismic waves and ground movements for SMART-1 array data. Earthquake Engineering and Structural Dynamics 1985;13:561–581.
[25] Loh CH. Spatial variability of seismic waves and its engineering application. Structural Safety 1991;10:95–111.
[26] Loh CH, Penzien J, Tsai YB. Engineering analysis of the SMART 1 array recordings. Earthquake Engineering and Structural Dynamics 1982;10(4):575–591.
[27] Loh CH, Yeh YT. Spatial variation and stochastic modelling of seismic differential ground movement. Earthquake Engineering and Structural Dynamics 1988;14(6):891–908.
[28] Papageorgiou AS, Aki K. A specific barrier model for the quantitative description of inhomogeneous faulting and the prediction of strong ground motion. I description of the model. Bulletin of the Seismological Society of America 1983;73(3):693–722.
[29] Sato H. Attenuation and envelope formation of three-component seismograms of small local earthquakes in randomly inhomogeneous lithosphere. Journal of Geophysical Research 1984;89(B2):1221–1241.
[30] Shinozuka M, Deodatis G. Stochastic process models for earthquake ground motion. Probabilistic Engineering Mechanics 1988;3(3):114–123.
[31] Shinozuka M, Deodatis G. Simulation of stochastic processes by spectral representation. Applied Mechanics Reviews, ASME 1991;44(4):191–204.
[32] Shinozuka M, Deodatis G. Simulation of multi-dimensional gaussian stochastic fields by spectral representation'. Applied Mechanics Reviews, ASME 1996;49(1):29–53.
[33] Theoharis AP. Wave representation of seismic ground motion. Ph.D. Dissertation, Department of Civil Engineering and Operations Research, Princeton University, NJ, 1991.
[34] Toksoz MN, Dainty AM, Charrette EE. Spatial variation of ground motion due to a lateral heterogeneity. Structural Safety 1991;10(1–3):53–77.
[35] Zeng Y. Deterministic and stochastic modeling of the high frequency seismic wave generation and propagation in the lithosphere. Ph.D. Dissertation, University of Southern California, Los Angeles, CA, 1991.
[36] Zeng Y, Aki K, Teng TL. Mapping of the high frequency source radiation for the Loma Prieta earthquake, California. Journal of Geophysical Research 1993;98(B7):11981–11993.
[37] Zerva A, Ang AH-S, Wen YK. Development of differential response spectra for lifeline seismic analysis. Probabilistic Engineering Mechanics 1986;1(4):208–218.
[38] Zhang R. Stochastic seismic ground motion modeling with imperfectly stratified earth medium. Journal of Sound and Vibration 1994;176(1):69–92.

[39] Zhang R. Statistical estimation of earthquake ground motion characteristics. Proceedings of 11th World Conference on Earthquake Engineering, Acapulco, Mexico, 23–28 June 1996, on CD-ROM.

[40] Zhang R, Deodatis C. Seismic ground motion synthetics of the 1989 Loma Prieta earthquake. International Journal of Earthquake Engineering and Structural Dynamics 1996;25(5):465–481.

[41] Zhang R, Zhang L, Shinozuka M. Seismic waves in a laterally inhomogeneous layered Medium. I: Theory. ASME Journal of Applied Mechanics 1997;64(1):50–58.

[42] Zhang R, Zhang L, Shinozuka M. Seismic waves in a laterally inhomogeneous layered Medium. II: Analysis. ASME Journal of Applied Mechanics 1997;64(1):59–65.

[43] Zhang R, Shinozuka M. Effects of irregular boundaries in layered half-space on seismic waves. Journal of Sound and Vibration 1996;195(1):1–16.

[44] Zhang R, Shinozuka M. On near-field earthquake ground motion simulation and its effects on long-period structures. Proceedings of Fourth National Workshop on Bridge Research in Progress, Buffalo, NY, 1996:71–76.